https://doi.org/10.17221/57/2022-SWR

Developing a decision-making model for improving the groundwater balance to control land subsidence

Mojtaba Zangeneh, Mahdi Sarai Tabrizi, Amir Khosrojerdi, Ali Saremi*

Department of Water Engineering and Sciences, Science and Research Branch, Islamic Azad University, Tehran, Iran

**Corresponding author: m.sarai@srbiau.ac.ir*

Citation: Zangeneh M., Sarai Tabrizi M., Khosrojerdi A., Saremi A. (2023): Developing a decision-making model for improving the groundwater balance to control land subsidence. Soil & Water Res., 18: 55–65.

Abstract: This study aimed to control land subsidence by improving the groundwater balance in the Varamin plain using the Groundwater Modelling System software and a multi-criteria decision model. For this purpose, aquifer level quantification and subsidence rate simulation were performed with the MODFLOW model and SUB package, respectively. The results showed a 6 m decrease in the aquifer level over a 5-year period and the subsidence rate in the central parts was 37 cm. Accordingly, the aquifer was evaluated by considering eight different restoration strategies based on reduced exploitation and artificial feeding. The results showed that the environmental criterion related to the subsidence adjustment index had the highest weight (0.27) and was introduced as the most important decision-making criterion. The evaluation of the results and priorities using the Complex Proportional Assessment (COPRAS) method showed that a 30% reduction in exploitation with artificial feeding is the best restoration strategy and can improve the subsidence rate and aquifer level by 36% and 76%, respectively, over a 5-year period (2024).

Keywords: COPRAS method; GMS software; MODFLOW; SUB package; SWARA method

In recent decades, the over-exploitation of groundwater and the improper management in the supply and demand of water resources have led to serious problems in water resources and the environment. Subsidence is an environmental problem that can be caused by oxidation of organic soils (Nieuwenhuis & Schokking 1997), sinkholes (Strzalkowski & Tomiczek 2015), mineral cavities (Deverel & Rojstaczer 1996; Choi et al. 2009; Al Heib et al. 2014), and the consolidation of geological structures due to groundwater depletion (Jafari et al. 2016). Extensive studies have been conducted on the relationship between the land subsidence and groundwater loss (Pacheco-Martínez et al. 2013; Ghenai et al. 2020; Noorbeh et al. 2020), and the results have indicated a high correlation. Shemshaki et al. (2007) simulated the land subsidence in the southwest plain of Tehran based on data from 1984 to 2012 and predicted that the subsidence rate would reach 33 cm by 2018. Therefore, the present study was performed to predict the amount of subsidence in the Varamin plain to develop a programme to stop this destructive process. The Varamin aquifer is highly exploited with no proper planning, and the reservoir deficit is significantly increasing each year. An important tool for evaluating this issue is the use of numerical models and examining different scenarios. Studies conducted in recent years using the PLAXIS, PFC2D and Groundwater Modelling System (GMS) numerical models with finite difference and finite element methods have shown the subsidence status of the earth. However, given the relationship between groundwater abstraction and subsidence, the use of the MODFLOW model to quantitatively simulate the aquifer and the SUB package to simulate the amount of subsidence could properly determine this relationship. Moreover, due to the need to plan and develop a decision-making model to apply aquifer equilibrium scenarios, it is important to use a numerical model to examine the subsidence rate in different scenarios

https://doi.org/10.17221/57/2022-SWR

and develop decision indicators. Therefore, the present study was aimed to develop a multi-criteria decision model based on the stakeholders in the study area using the aquifer subsidence control approach.

MATERIAL AND METHODS

Characteristics of the study area

The Varamin plain with an area of 1 595 km^2 located at the geographical coordinates 55°3' to 56°8'E and 28°5' and 29°6'N has an unconfined alluvial aquifer (Figure 1). The water resources in this region have always been affected by the upstream activities due to the shape of the aquifer, the physical boundaries of the Varamin plain, and the flow pattern. Examinations of the balance of the groundwater resources of this region shows that, given the water transfer plans to control the groundwater depletion, this aquifer is facing a negative balance and has a reservoir deficit of more than 90 million cubic metres per year. Given the balance condition and the presence of clay layers, subsidence in this region causes environmental problems, which are serious due to the irreversibility of the phenomenon. Figure 1 provides an overview of the study area and the composition of the geological formations. The boundary conditions of the model were determined based on the inflow and outflow network to the aquifer based on the inflow and outflow to the aquifer based on 320 inlet and 153 outlet sections within the Varamin Plain aquifer. Based on this, the total amount of underground inflow and outflow in the water year 2014–2015 was calculated and estimated as 116.1 and 41.43 million cubic meters, respectively. Based on this, in this water year, 74.64 million cubic meters of water will be stored in the aquifer by the border streams.

Research method. After investigating the study area, the groundwater flow and the subsidence rate were simulated using by the MODFLOW model and the SUB package by GMS (Ver. 10) software. The satellite images and subsidence rate during the simulation period were also used to calibrate the results and accurately estimate the soil elasticity coefficients in the aquifer. After finalising the flow and aquifer subsidence models, the aquifer restoration strategies were simulated according to the exploitation policies of the region. Finally, the restoration strategies were evaluated and prioritised using a decision-making model based on economic, social, environmental, and technical criteria to control the subsidence (Zangeneh et al. 2021).

Preparation of the quantitative model of the aquifer. The aquifer model, based on the squared grid scale of 500 m, utilises a finite difference approach. Given the balance of the groundwater resources, the amount of recharge to the aquifer (returned and infiltrated water from rainfall, runoff and agricultural drained water), the utilisation of the groundwater resources, the evaporation of the groundwater, the inflow and outflow of the aquifer, the surface water

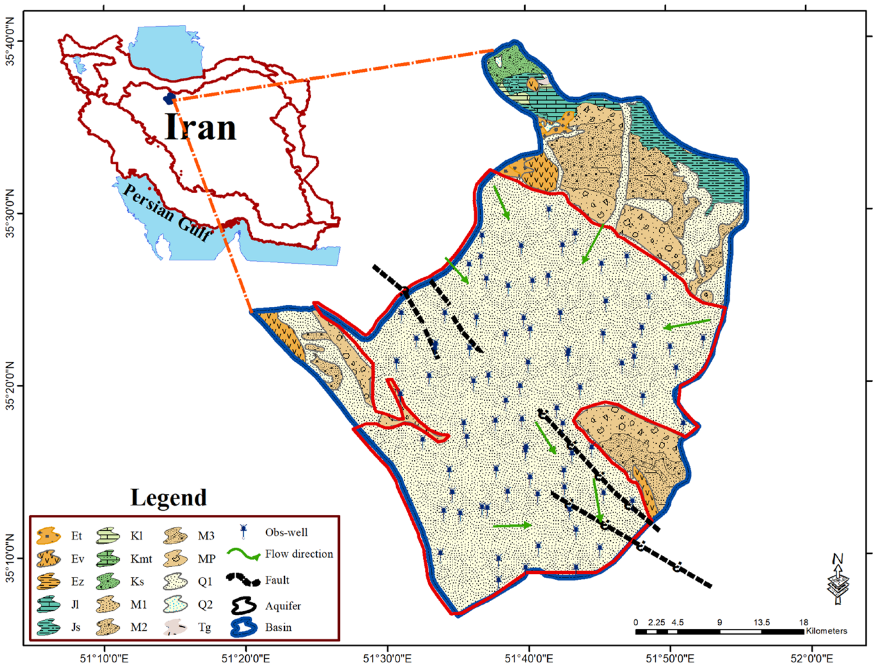

Figure 1. View of the study area

https://doi.org/10.17221/57/2022-SWR

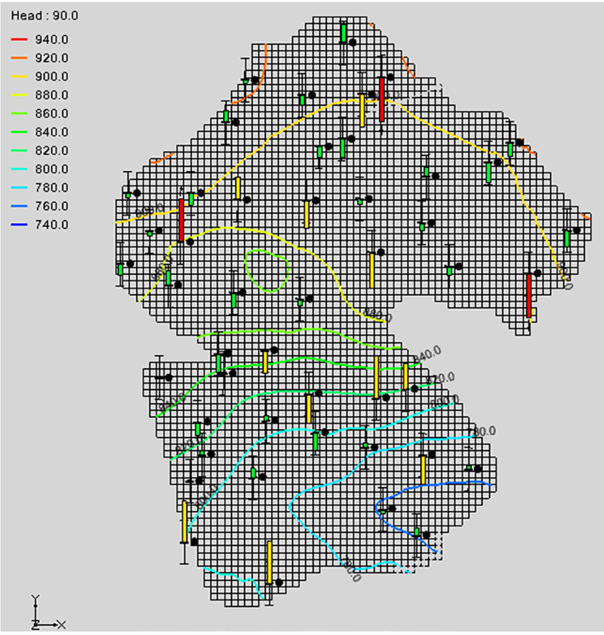

Figure 2. View of the final model of the unsustainable groundwater flow

bodies, and the drainage of the region were included in the model. Due to the existence of the aquifer in the area, observation wells of the area were defined separately in the model. After preparing the conceptual model of the aquifer, its structure, i.e., the topography of the land, the initial level of the groundwater, and the bedrock in the aquifer, were included in the model. The topography of the area from the digital elevation model (DEM), the initial groundwater level based on the observation wells and the bedrock based on the geophysical results of the zoning area and as an aquifer structure were entered into the model. The hydrodynamic parameters of the aquifer, including the hydraulic conductivity, storage coefficient, and specific aquifer discharge, were also extracted based on the results of pumping experiments in the area and were introduced as initial values in the model (Aqebatbekheyr et al. 2021). After preparing the conceptual model of the aquifer, it was simulated for a period of six years (2014–2019) with unsteady flow. At the first step, the model was calibrated with steady flow October 4, 2014. The 24 season steps were considered for the simulation. After the initial simulation, the quantitative model of the aquifer, as well as its hydraulic conductivity and specific yield, as calibration variables in the steady and unsteady state, were calibrated. Afterward, the validation was performed based on changes in the aquifer behaviour in the last year of the simulation period. Figure 2 shows the simulated groundwater level in the quantitative aquifer model.

Subsidence simulation. After the quantitative simulation of the aquifer, the SUB package was used to simulate the amount of land subsidence due to water abstraction. In this type of modelling, the geostatic pressure is considered a function of the groundwater level, and the density is considered a function of the effective pressure changes in the bedrock (Pacheco-Martínez et al. 2013).

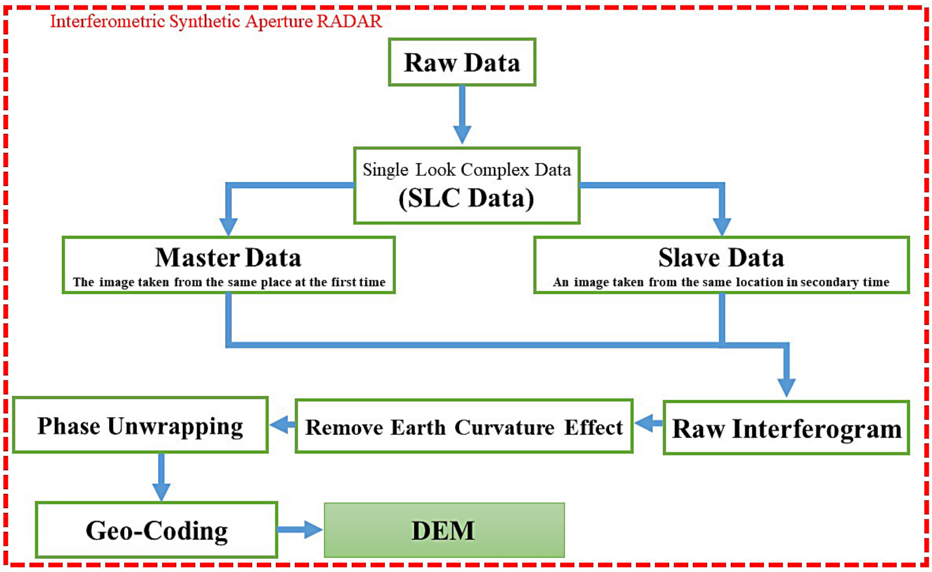

Figure 3. Steps to perform the radar interference
DEM – digital elevation model

https://doi.org/10.17221/57/2022-SWR

Satellite images. The radar interferometry method was used to measuring the subsidence process based on its high capability of spatial distribution, simplicity, and ease of implementation, along with its low cost. The images extracted from the Sentinel-1 satellite were used to measure and monitor the subsidence since 2014 (Keršuliene et al. 2010). This method is based on the difference in the measurement of the radar images taken from an area. Accordingly, the steps for performing radar interference are described in Figure 3. Given the variety of imaging modes of the satellite sensor, the IW (Interferometric Wide Swath) method was used for the radar interference. The width of the images was 250 km with a spatial separation of 5 m along the azimuth and 20 m along the domain.

Development of the multi-criteria decision model (MCDM)

In this study, in order to investigate the effects of the selected restoration solution in the region, the defined criteria are first ranked using the Stepwise Weight Assessment Ratio Analysis (SWARA) method, and in the next step, their weighting is performed using the Complex Proportional Assessment (COPRAS) method. To begin with, the criteria were ranked according to their importance, taking the purpose of the research into account. The SWARA technique is used for weighting influencing parameters and the COPRAS technique is used as a multi-criteria decision making model. Moreover, the SWARA technique is used for weighting, influencing the technical, environmental and social criteria.

SWARA method. The SWARA method was developed by Cresol in 2010. The SWARA method ranks the criteria according to the opinions of experts (García-Cascales & Lamata 2012). The process of weighting the criteria by SWARA is as follows:

Step 1: Sort the criteria in a descending order based on the opinions of experts

Step 2: Determine the relative importance of each criterion relative to the criterion above itself (S_j)

Step 3: Calculate the relative importance of each criterion (k_j)

$$k_j = \begin{cases} 1 & j = 1 \\ S_j + 1 & j > 1 \end{cases} \quad (1)$$

Step 4: Determine the recalculated weight (q_j)

$$q_j = \begin{cases} 1 & j = 1 \\ \dfrac{q_{j-1}}{k_j} & j > 1 \end{cases} \quad (2)$$

Step 5: Determine the final weight of the criteria (w_j)

$$w_j = \frac{q_j}{\sum_{k=1}^{n} q'_k} \quad (3)$$

where:

w_j – the standard weight of criterion j;

n – the number of criteria;

k – the relative importance value of each criterion.

COPRAS method. The COPRAS method is new multi-criteria decision-making (MCDM) approach proposed by Zavadskas et al. (2010). The following steps are used to rank the options using the COPRAS method:

(1) Determine the weights of the criteria using a common method, such as Shannon entropy or hierarchical process.

(2) Form a decision matrix (a decision matrix is a list of values in rows and columns that allows an analyst to systematically identify, analyse, and rate the performance of relationships between sets of values and information. Elements of a decision matrix show decisions based on certain decision criteria.)

(3) Normalise and weigh the decision matrix using the following equation:

$$d_{ij} = \frac{w_j}{\sum_{j=1}^{n} x_{ij}} x_{ij} \quad (4)$$

where:

d_{ij} – coefficient for determining the weight of the criteria;

x_{ij} – the value of each option per criterion (decision-making options are measured with ranking indicators to select the best measure. In such a way that first weighting the criteria with method 2 and then ranking it with method 1 makes it possible to easily choose the best management criteria and indicators.).

After determining the positive and negative criteria, their final values must be determined, using Equation (5):

$$S_j^- = \sum_{z_i} = -d_{ij}$$
$$S_j^+ = \sum_{z_i} = +d_{ij} \quad (5)$$

where:

z_i – the value of each of the technical, social, economic and environmental criteria.

Equation (6) is used to calculate the final value of each Q option.

https://doi.org/10.17221/57/2022-SWR

$$Q_i = S_j^+ + \frac{S_{\min}^- \sum_{j=1}^n S_j^-}{S_j^- \sum_{j=1}^n \frac{S_{\min}^-}{S_j^-}} = S_j^+ + \frac{\sum_{j=1}^n S_j^-}{S_j^- \sum_{j=1}^n \frac{1}{S_j^-}} \quad (6)$$

In this equation, S_j^+ and S_j^- equal the algebraic sum of the positive and negative criteria for each option, respectively. The following equation gives the percentage of points of each option:

$$N_i = \frac{Q_i}{Q_{\max}} \times 100\% \quad (7)$$

RESULTS

Groundwater modelling

Quantitative status of the aquifer. The aquifer hydrodynamic parameters include the hydraulic conductivity, aquifer special storage and discharge coefficient, which are also based on the results of the extraction area pumping experiments and provided in the form of initial values in the entered model. Then, the values of these parameters are corrected in the intermediary and the accuracy of the model under steady and unsteady flow conditions. The steady flow state model was selected and recalibrated September 2014, and, after that, the unsteady state flow model was simulated and subjected to recalibration and verification for 5 years (Figure 5). The calibration and verification procedures were stopped as the root mean square error (RMSE) reached less than 0.05 m and 0.25 m, respectively. The model simulations have been performed daily (daily time steps). The model calibration for the steady flow condition was undertaken for one month in September 2014 and for five years (2014–2019) for the unsteady flow condition and, finally, the model verification was undertaken with the data of 2020, which is a year outside the model calibration period. The boundaries of the Varamin Plain aquifer are divided into three types, which were well considered in the modelling, which include: (A) Impermeable boundaries, (B) Permeable boundaries with a certain hydraulic load and (C) Permeable boundaries with a known value.

Table 1 exhibits the balance components of the Varamin aquifer in full. The northern part of the aquifer forms the incoming groundwater flow and the south-eastern part of the aquifer forms the outgoing groundwater flow. The maximum thickness of the Varamin alluvial aquifer is about 305 metres at the entrance of the Jajrood river to the Varamin plain, which is actually the result of the sedimentation of materials transported to this area. The low level of the bedrock at this point can be seen as the result of the Parchin fault (slope component), which caused the Miocene formations to fall, and, as a result, formed a depression that was accumulated by the Jajrood river during the subsequent epochs.

Table 2 presents the states of aquifer groundwater level in the model in the steady and unsteady state. The region's geological formation information and the results of the pumping experiments were used to calibrate the model. The upper parts of the aquifer had larger grains and higher hydraulic conductivity, while the middle and lower parts had finer grains and lower hydraulic conductivity. Moreover, the hydraulic conductivity had a high correlation with the special discharge in the aquifer, and, as a general trend, the specific discharge decreased from the inflow to the outflow of the aquifer. Figure 4 illustrates the simulation and the differences between

Table 1. Balance of groundwater resources of the Varamin aquifer (in MCM) (Ministry of Energy 2019)

The extent of the aquifer (km^2)		104.30
Aquifer recharge	inside groundwater entering the aquifer	30.91
	infiltration from aquifer surface rainfall	10.68
	infiltration from surface run off	23.50
	infiltration from agricultural water	259.88
	infiltration from drinking water and industry	54.69
Aquifer discharge	discharge from wells, aqueducts and springs	447.38
	natural and artificial drainage	3.50
	evaporation from the aquifer	4.47
	outside groundwater from the aquifer	15.97
Storage volume changes		–91.93

MCM – million cubic metres

https://doi.org/10.17221/57/2022-SWR

Table 2. The amounts of the technical, economical, and subsidence control indices using the eight aquifer restoration strategies

BS	MS	YRR (%)	The groundwater level (m)		Index (%)	Subsidence in 2024 (m)			Land subsidence control index (%)	Government expense	Exploitation costs	Total cost	Normalised cost ratio
			2019	2024		max	min	average		(billion Rials)			
Reduction in the exploitation	A_1	5	874.7	873.4	10.4	35	7	20.1	6.2	8.8	5.464	14.264	0.31
	A_2	10		872.3	21.9	32	7	19.5	15.4		10.928	19.728	0.43
	A_3	20		870.5	41.1	27	7	17.9	40		21.856	30.656	0.66
	A_4	30		867.8	69.3	25	6.5	17.2	50.8		32.784	41.584	0.90
Reduction in the exploitation + artificial recharge	A_5	5		873.2	13	34	7	19.7	12.3	13.5	5.464	18.964	0.41
	A_6	10		872.0	24	31	7	19.1	21.5		10.928	24.428	0.53
	A_7	20		870.1	45.3	26	7	17.4	47.7		21.856	35.356	0.76
	A_8	30		866.9	76	23.5	6.2	16.8	56.9		32.784	46.284	1

BS – balance solution; MS – managerial scenario; YRR – yield reduction rate

the groundwater levels in the steady model after calibration. According to the results, five observation wells had the highest differences between the observed and simulated groundwater levels. Wells 28, 49, and 73 showed the highest water elevation, while wells 66 and 71 showed the highest groundwater depletion. Examination of the network of observation wells of the Varamin aquifer showed that the simulation error was acceptable in most wells. Figure 5 indicates the final analysis of the steady state and unsteady state model of the groundwater flow in the aquifer after calibration. After validating the model and evaluating the acceptable correlation between the observed and simulated groundwater levels, the future status of the aquifer was predicted, assuming the continuation of the current situation for five years. For this purpose, the normal climatic conditions and the existing exploitation conditions were considered.

Subsidence based on satellite images. Figure 6A shows the amount of land subsidence in the six-year period. The results showed that the highest land subsidence in the Varamin aquifer during the mentioned period was 23 cm, which happened in the central part of the aquifer, which had the deepest wells. In general, the areas with the most wells and the areas with the outflow have the highest rate of subsidence. Compressible layers of clay gain more specific gravity by absorbing water, leading to a decrease in the aquifer and groundwater level. In the subsidence model for the period of unsteady conditions, the pre-consolidation head coefficients were estimated by the raw data and interpolation method. Accordingly, the model results and the coefficients of pre-reinforcement head or stress, elastic coefficient, inelastic coefficient, and initial density were calibrated by trial and error. The values of the compression coefficients were determined and calibrated using drilling logs to obtain the compressible layers in the aquifer. The pre-consolidation coefficient was found to be between 860 and 970 metres. The pre-pre-consolidation head was obtained equal to the initial groundwater level considered by the model. On the other hand, according to the US Geological Survey (Leake & Galloway 2010, 6-A23), the inelastic and elastic coefficient ranges in the aquifer were considered to be 0.003–0.05 and 0.02–0.04, respectively. The subsidence simulation showed that the central parts of the aquifer, which currently have a great deal of subsidence, will continue to subside and will reach a maximum of 37 cm by 2024. Figure 6B shows the zoning of the aquifer in 2024. The average aquifer

https://doi.org/10.17221/57/2022-SWR

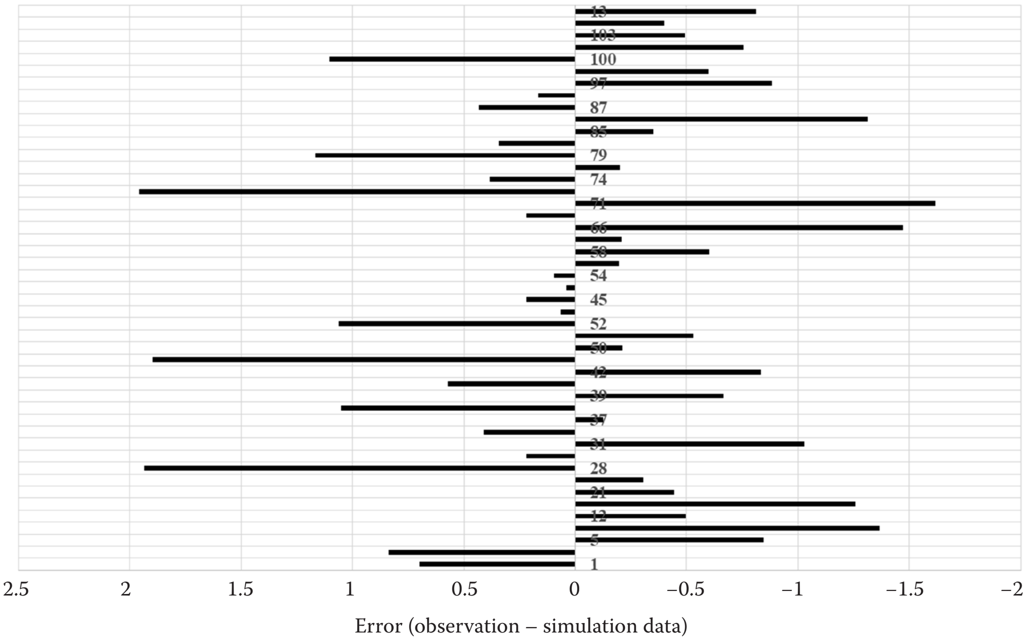

Figure 4. The difference between the simulated and observed groundwater levels in the observation wells in the steady model

subsidence in 2024 was estimated at 20.5 cm with a minimum of 7 cm (aquifer exit) and a maximum of 37 cm (central aquifer).

Groundwater management strategies for the aquifer restoration. Based on the simulated aquifer subsidence, two strategies were considered to reduce the water abstraction and increase the aquifer recharge. Accordingly, the following groundwater management alternatives were selected for the restoration of the Varamin aquifer:

A1: 5% reduction in the groundwater abstraction, A2: 10% reduction in the groundwater abstraction, A3: 20% reduction in the groundwater abstraction, A4: 30% reduction in the groundwater abstraction, A5: A1 + artificial feeding, A6: A2 + artificial feeding, A7: A3 + artificial feeding, and A8: A4 + artificial

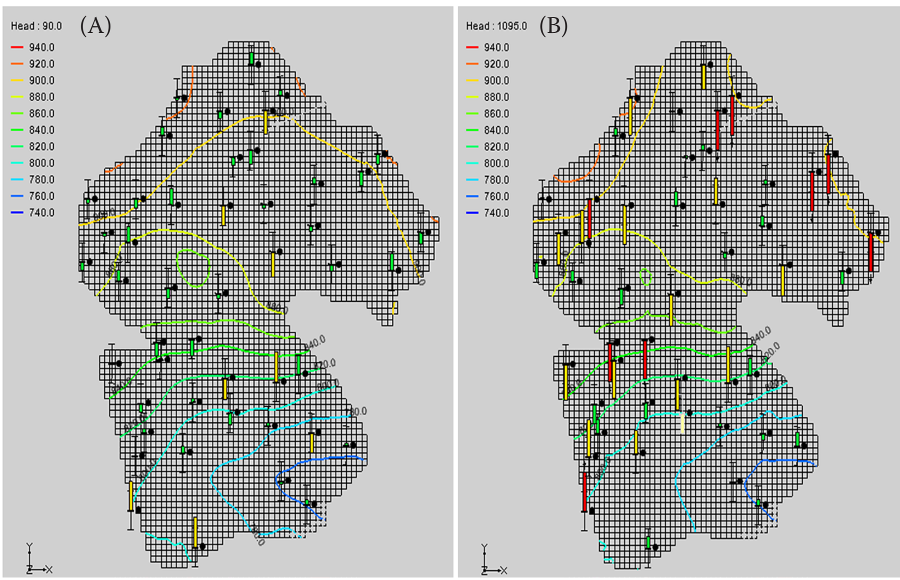

Figure 5. The final model of the quantitative state in the Varamin aquifer, steady model (A) and unsteady model (B)

https://doi.org/10.17221/57/2022-SWR

feeding. Then, a multi-criteria decision-making model was developed to examine the different dimensions of the problem. Accordingly, the technical (C1), economic (C2), social (C3), and environmental (C4) criteria were introduced to evaluate the restoration strategies. The aquifer quantitative improvement index (C1) was introduced as a technical index indicating the relative changes in the groundwater level in each solution. By using this index, the ratio of the increase or decrease in the groundwater level during the forecast period was examined in comparison with the beginning of the forecast period. Equation (8) shows this index:

$$\alpha_{Gl} = \sum_{i=1}^{n} \left(\frac{Gl_{sc} - Gl_{2024}}{Gl_{2019} - Gl_{2024}} \right) \times 100 \tag{8}$$

where:

α_{Gl} – the index of the groundwater level improvement (%);

Gl_{2024} – the groundwater level (m) in 2024 without applying any scenario;

Gl_{2019} – the groundwater level (m) at the beginning of 2019;

n – the number of the model cell;

Gl_{sc} – groundwater level (m) in the case of applying a restoration solution.

Table 2 lists the technical, economical, and subsidence control indices of the groundwater level improvement using the eight restoration strategies. The groundwater level in 2024, without applying any strategy and in the current similar conditions, will be 855.5 m. The results showed that solution A8 would have the greatest improvement in the quantitative status of the aquifer. However, there was no significant difference between the A8 and A4 managerial scenarios.

Unfortunately, based on a national plan titled "Restoration and balancing of the country's groundwater resources", due to the serious problems with the significant drop in the level of the groundwater in almost most of the country's plains, in addition to monitoring artificial recharging costs, the government pays for the costs of monitoring the pumping and distribution of groundwater and blocking unauthorised wells. slowly so that the groundwater level in the water table rises and the aquifers find relatively stable conditions in order to finally prevent dangerous environmental consequences including subsidence, dust and fine dust and forced migrations, etc., which may occur due to the instability of the aquifer. An economic evaluation was conducted based on the cost that the government incurs to implement each solution, and the amount of funds that would reduce the user revenue. The government costs are related to the projects considered for the implementation and careful monitoring of groundwater extraction and artificial recharge, which is conducted with the help of patrol and inspection teams located in the water affairs departments of each region. Farmers' expenses

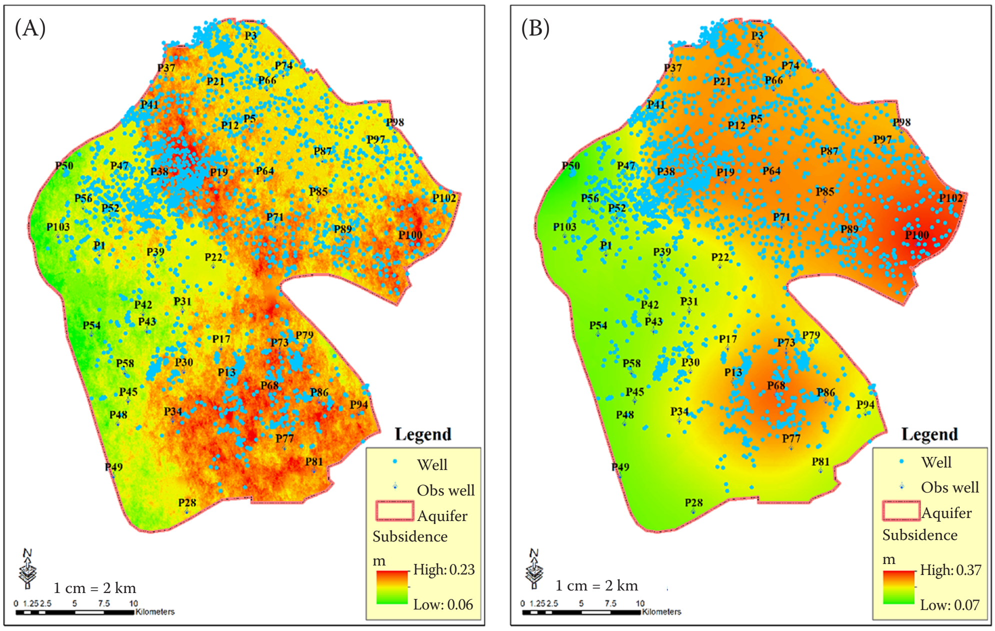

Figure 6. The land subsidence of the Varamin Aquifer in 2019 (A) and 2024 (B)

https://doi.org/10.17221/57/2022-SWR

Table 3. Weighting of the criteria by the Stepwise Weight Assessment Ratio Analysis (SWARA) method

Symbol	Criterion	Importance of comparative mean value (S_j)	Coefficient $k_j = s_j + 1$	Recalculated weight $q_j = q_{j-1}/k_j$	Weight $w_j = q_j/\Sigma q_j$
C_4	environmental	–	1	1	0.27
C_2	economic	0.097	1.097	0.91	0.242
C_3	social	0.088	1.088	0.92	0.244
C_1	technical	0.075	1.075	0.93	0.25
Total				3.8	1

related to the reduction of the exploitation, fines for excess harvesting and purchase of control equipment such as a smart meter, well equipment and repairs, etc. are also considered. These costs were estimated with the cooperation of regional water experts and agricultural activists in the region. All the costs (C) were normalised using Equation (9) (Table 3):

$$C = 1 - \frac{C_{\max} - C_i}{C_{\max}} \quad (9)$$

where:

$C_{\max}$ – the maximum cost of the restoration options;

C_i – the cost of each technical criterion.

In order to evaluate the social satisfaction index, a field survey was conducted among the region's water consumers using a questionnaire focused on justice in water allocation and equality in reducing exploitation. A critical issue regarding the management scenarios was the great dependence of the people of the region on agricultural production. They blamed the government for such problems and expected a great deal of support from the public sector. The highest level of satisfaction (68%) belonged to solution A5 (5% reduction in exploitation, along with artificial nutrition), while the lowest level of satisfaction (6%) was associated with solution A4.

Given the definition of the eight solutions to improve the existing conditions, the landslide control index was defined as Equation (10). This index is expressed as a percentage and evaluates the improvement of landslides compared to 2019 due to the implementation of restoration strategies.

$$\gamma = 100 \times \left(\frac{\alpha_{2024} - \alpha_{Sc}}{\alpha_{2024} - \alpha_{2019}} \right) \quad (10)$$

where:

γ – the subsidence control index (%);

α_{Sc} – the subsidence (m) under the conditions of adopting a solution;

α_{2019} – the subsidence (m) at the beginning of the forecast period;

α_{2024} – the subsidence (m) at the end of the forecast period.

The land subsidence control index calculated based on the simulations is shown in Table 4. Accordingly, the greatest improvement in the quantitative status of the aquifer (the highest reduction in the land subsidence) was made by solution A8.

Multi-criteria decision-making models. To select the best restoration strategy in the first region, the four defined criteria were ranked using the SWARA method and then weighted by the COPRAS method. In the first stage, the criteria were ranked based on the degree of importance according to the opinion of 15 experts. In the next steps, the coefficients k_j and q_j and the weight of the criteria were calculated. The results of SWARA showed that the environmental criterion, at 0.27, was more important than the other criteria. The technical and social criteria were also ranked next with weights of 0.25 and 0.244, respectively. The economic criterion with a weight of 0.242 was the least important criterion.

Table 4. The results of the ranking of solutions

Solution	S_i^+	S_i^-	Q	N (%)	Ranking
A_1	0.07	0.02	0.125	76.5	4
A_2	0.07	0.02	0.108	66.2	7
A_3	0.09	0.03	0.117	71.7	6
A_4	0.12	0.04	0.141	86.2	2
A_5	0.09	0.02	0.131	80.4	3
A_6	0.09	0.03	0.120	73.9	5
A_7	0.11	0.04	0.131	80.4	3
A_8	0.14	0.05	0.153	94.1	1

S_i^+ – mean value values of positive criteria for each restoration strategy; S_i^- – mean value values of negative criteria for each restoration strategy; Q – relative importance value; N – the performance index

https://doi.org/10.17221/57/2022-SWR

After determining the weight of the criteria, using the COPRAS method, the strategies to adjust the aquifer subsidence rate were prioritised. For this purpose, after preparing the initial matrix by the Shannon entropy method, the criteria were normalised and weighted based on Equations (9) and (10) of the decision matrix. According to the cost discussion, the economic criterion was considered as a negative indicator and three technical, environmental and social criteria were considered positive. The positive (S_i^+) and negative (S_i^-), relative importance (Q_i) and performance index (N_i) were obtained for each restoration strategy. Strategies were ranked based on the Q_i and N_i values and the performance index of each was determined according to its rank. So that high values of Q_i and N_i for a strategy equals its higher rank. The results listed in Table 4 indicate that solution A8 had the highest relative importance compared to the other options, so it was ranked first. This solution included a 30% reduction in pumping from the aquifer along with the artificial feeding of the groundwater.

The study of the priorities showed that despite the low level of the social satisfaction in the A8 solution, the higher weight of the environmental criterion due to the rate of land subsidence and the improvement of the aquifer quantitative status made this method a priority. Figure 7 demonstrates the quantitative recovery of the aquifer based on the trend of the water table and the reduction of the subsidence by zoning the results obtained for the A8 restoration strategy. The study on land subsidence in the Varamin aquifer showed that adopting a solution decreased the degree of the subsidence continuity and reduced the high level of subsidence in the central parts of the aquifer compared to the 2024 forecast. Moreover, the statistical study on the exploitation areas and the subsidence indicated a direct relationship so that the sectors that still had relatively high land subsidence were concentrated in the areas with the high volume of exploitation.

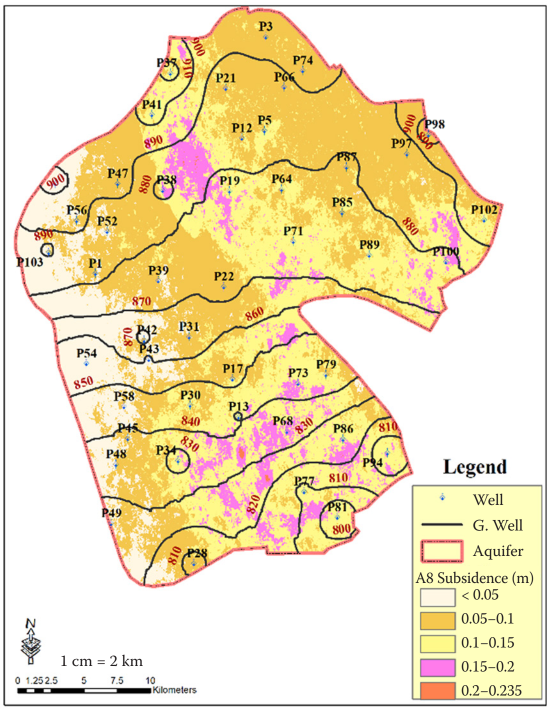

Figure 7. Subsidence and groundwater level improvement after the adoption of solution A8

CONCLUSION

The land subsidence rate in the Varamin plain of Tehran based on the available data was predicted to reach about 33 cm. Therefore, the present research was conducted to predict the amount of subsidence in the mentioned plain. Furthermore, this study evaluated the restoration strategies of the Varamin aquifer using the SWARA-COPRAS decision-making model. Accordingly, the technical, economic, social, and environmental criteria were defined to analyse the groundwater level, the costs of implementing the restoration strategies, social satisfaction, and the extent of the landslide control. The results of the weighting the criteria showed that the environmental criterion, which was related to the land subsidence control index, had the highest weight with a value of 0.27; so, it was introduced as the most important criterion in the decision-making. The evaluation of the results and priorities of the solutions using the COPRAS method revealed that a 30% reduction in the groundwater abstraction with artificial feeding was the first priority for the aquifer restoration. The results showed that adopting this solution would reduce the land subsidence so that the maximum amount of subsidence would be 23.5 cm in the central parts of the aquifer. The quantitative status of the aquifer was also improved by 76% compared to the forecast period (2024).

REFERENCES

Al Heib M., Duval C., Theoleyre F., Watelet J.M., Gombert P. (2014): Analysis of the historical collapse of an abandoned underground chalk mine in 1961 in Clamart

(Paris, France). Bulletin of Engineering Geology and the Environment, 74: 1001–1018.

Aqebatbekheyr H., Sarai Tabrizi M., Kardan Moghaddam H. (2021): Assessing the effects of volcanoes on the qualitative changes of groundwater resources using quantitative and qualitative modeling of Khash aquifer. Iranian Journal of Water Research, 39: 141–152.

Choi J.K., Kim K.D., Lee S., Won J.S. (2009): Application of a fuzzy operator to susceptibility estimations of coal mine subsidence in Taebaek City, Korea. Environmental Earth Sciences, 59: 1009–1022.

Deverel S.J., Rojstaczer S. (1996): Subsidence of agricultural lands in the Sacramento-San Joaquin Delta, California: Role of aqueous and gaseous carbon fluxes. Water Resources Research, 32: 2359–2367.

García-Cascales M.S., Lamata M.T. (2012): On rank reversal and TOPSIS method. Mathematical and Computer Modelling, 56: 123–132.

Ghenai C., Albawab M., Bettayeb M. (2020): Sustainability indicators for renewable energy systems using multi-criteria decision-making model and extended SWARA/ARAS hybrid method. Renewable Energy, 146: 580–597.

Jafari F., Javadi S., Golmohammadi G., Karimi N., Mohammadi K. (2016): Numerical simulation of groundwater flow and aquifer-system compaction using simulation and InSAR technique: Saveh basin, Iran. Environmental Earth Sciences, 75: 1–10.

Keršuliene V., Zavadskas E.K., Turskis Z. (2010): Selection of rational dispute resolution method by applying new step-wise weight assessment ratio analysis (SWARA). Journal of Business Economics and Management, 11: 243–258.

Leake S.A., Galloway D.L. (2010): Use of the SUB-WT Package for MODFLOW to simulate aquifer-system compaction in Antelope Valley, California, USA. In: Land Subsidence, Associated Hazards and the Role of Natural Resources Development: Proc. 8th Int. Symposium on Land Subsidence: Queretaro, Oct 17–22, 2010: 61–67.

Ministry of Energy (2019): Water Resources Balance Update Studies in the Study Area of the Namak Lake Basin. Balance Report No. 4134. Birjand, Department of Basic Studies of Water Resources Management Company.

Nieuwenhuis H.S., Schokking F. (1997): Land subsidence in drained peat areas of the Province of Friesland, The Netherlands. Quarterly Journal of Engineering Geology and Hydrogeology, 30: 37–48.

Noorbeh P., Roozbahani A., Kardan Moghaddam H. (2020): Annual and monthly dam inflow prediction using bayesian networks. Water Resources Management, 34: 2933–2951.

Pacheco-Martínez J., Hernandez-Marín M., Burbey T.J., González-Cervantes N., Ortíz-Lozano J.Á., Zermeño-De-Leon M.E., Solís-Pinto A. (2013): Land subsidence and ground failure associated to groundwater exploitation in the Aguascalientes Valley, México. Engineering Geology, 164: 172–186.

Shemshaki A., Boulourchi M.J., Entezam Soltani I. (2007): The study land subsidence in Tehran plain and its casual factors. In: 24th Earth Sciences Meeting, Geological Survey and Mineral Explorations of Iran, Tehran, July 10–11, 2007: 2018–2019.

Strzalkowski P., Tomiczek K. (2015): Analytical and numerical method assessing the risk of sinkholes formation in mining areas. International Journal of Mining Science and Technology, 25: 85–89.

Zangeneh M., Sarai Tabrizi M., Khosrojerdi A., Saremi A. (2021): Effectiveness of groundwater resources balancing strategies for landslide control (Case study: Varamin study area). Iranian Journal of Soil and Water Research, 52: 1735–1751.

Zavadskas E.K., Kaklauskas A., Vilutiene T. (2010): Multicriteria evaluation of apartment blocks maintenance contractors: Lithuanian case study. Vilnius Gediminas Technical University, 13: 319–338.

Received: April 13, 2022
Accepted: January 18, 2023
Online first: February 6, 2023